Molecular Biology of the Cell
Vol. 15, 234–244, January 2004

Tyrosine Phosphatase Epsilon Is a Positive Regulator of Osteoclast Function in Vitro and In Vivo

Riccardo Chiusaroli,*† Hilla Knobler,†‡ Chen Luxenburg,†§ Archana Sanjay,* Shira Granot-Attas,¶ Zohar Tiran,¶ Tsuyoshi Miyazaki,* Alon Harmelin,‖ Roland Baron,*# and Ari Elson¶#

*Departments of Cell Biology and Orthopedics, Yale University School of Medicine, New Haven, Connecticut 06510; ‡Metabolic Unit, Kaplan Medical Center, Rehovot, Israel; and Departments of §Molecular Cell Biology, ¶Molecular Genetics, and ‖Veterinary Resources, The Weizmann Institute of Science, Rehovot 76100, Israel

Submitted April 6, 2003; Revised August 31, 2003; Accepted September 9, 2003
Monitoring Editor: Mary Beckerle

Protein tyrosine phosphorylation is a major regulator of bone metabolism. Tyrosine phosphatases participate in regulating phosphorylation, but roles of specific phosphatases in bone metabolism are largely unknown. We demonstrate that young (<12 weeks) female mice lacking tyrosine phosphatase epsilon (PTPε) exhibit increased trabecular bone mass due to cell-specific defects in osteoclast function. These defects are manifested in vivo as reduced association of osteoclasts with bone and as reduced serum concentration of C-terminal collagen telopeptides, specific products of osteoclast-mediated bone degradation. Osteoclast-like cells are generated readily from PTPε-deficient bone-marrow precursors. However, cultures of these cells contain few mature, polarized cells and perform poorly in bone resorption assays in vitro. Podosomes, structures by which osteoclasts adhere to matrix, are disorganized and tend to form large clusters in these cells, suggesting that lack of PTPε adversely affects podosomal arrangement in the final stages of osteoclast polarization. The gender and age specificities of the bone phenotype suggest that it is modulated by hormonal status, despite normal serum levels of estrogen and progesterone in affected mice. Stimulation of bone resorption by RANKL and, surprisingly, Src activity and Pyk2 phosphorylation are normal in PTPε-deficient osteoclasts, indicating that loss of PTPε does not cause widespread disruption of these signaling pathways. These results establish PTPε as a phosphatase required for optimal structure, subcellular organization, and function of osteoclasts in vivo and in vitro.

INTRODUCTION

Reversible phosphorylation of tyrosine residues in proteins is a central regulator of cellular functions and is a process controlled by the opposing actions of protein tyrosine kinases (PTKs) and tyrosine phosphatases (PTPs; Hunter, 1995). PTPs, which are molecularly, biochemically, and physiologically distinct from PTKs, are intimately involved in regulating the same processes although many details of how this is achieved are still unknown (Li and Dixon, 2000; Andersen *et al.*, 2001b; Tonks and Neel, 2001).

The protein tyrosine phosphatase epsilon (PTPε) subfamily contains four distinct proteins, all products of a single gene. The two major forms of PTPε are the receptor-type (RPTPε) and nonreceptor type (cyt-PTPε) isoforms (Krueger *et al.*, 1990; Elson and Leder, 1995a, 1995b; Nakamura *et al.*, 1996; Tanuma *et al.*, 1999). Two other forms of PTPε are p67 and p65 PTPε; these are shorter molecules, whose production is regulated at the levels of translation and posttranslational processing (Gil-Henn *et al.*, 2000, 2001). The four PTPε forms differ only at their amino termini, resulting in their unique subcellular localization patterns and distinct physiological functions. RPTPε assists Neu-induced mouse mammary tumor cells maintain their transformed phenotype, most likely by dephosphorylating and activating Src in vivo (Elson and Leder, 1995a; Elson, 1999; Gil-Henn and Elson, 2003). The same form of PTPε can also downregulate insulin receptor signaling in cultured cells (Moller *et al.*, 1995; Andersen *et al.*, 2001a). cyt-PTPε dephosphorylates and downregulates delayed-rectifier voltage-gated potassium channels in Schwann cells, correlating with delayed myelination of sciatic nerve axons in young PTPε-deficient mice (Peretz *et al.*, 2000). In some systems PTPε can downregulate mitogenic signaling, as exemplified by its inhibition of MAP kinase activity (Wabakken *et al.*, 2002; Toledano-Katchalski *et al.*, 2003) and inhibition of JAK-STAT signaling in M1 leukemia cells (Tanuma *et al.*, 2000, 2001, 2003). PTPε has also been shown to be important for proper function of macrophages (Sully *et al.*, 2001).

Tyrosine phosphorylation plays a major role in regulating bone structure and metabolism, suggesting that dysregulation of kinase-phosphatase equilibria may result in abnormalities in this organ system. Accordingly, mice genetically lacking Src or in which Src is inhibited pharmacologically are osteopetrotic due to severely reduced function of osteoclasts, the cells that degrade bone (Soriano *et al.*, 1991; Boyce *et al.*, 1992; Horne *et al.*, 1992; Lowe *et al.*, 1993;

Article published online ahead of print. Mol. Biol. Cell 10.1091/mbc.E03–04–0207. Article and publication date are available at www.molbiolcell.org/cgi/doi/10.1091/mbc.E03–04–0207.

Corresponding authors. E-mail addresses: roland.baron@yale.edu; ari.elson@weizmann.ac.il.

† These authors contributed equally to this work.

Abbreviations used: PTP, protein tyrosine phosphatase; cyt-PTPε, nonreceptor form of PTPε; *Ptpre−/−*; genetically lacking PTPε; OCL, osteoclast-like cell.

Missbach *et al.*, 1999; Violette *et al.*, 2000, 2001). Aberrant tyrosine phosphorylation can also be caused by changes in PTP activity, although little data to this effect is available in bone. Inhibition of the receptor-type phosphatase PTP-OC in cultured rabbit osteoclasts reduces their resorption activity (Wu *et al.*, 1996; Suhr *et al.*, 2001), whereas inhibition of OST-PTP abrogates differentiation of cultured osteoblasts (Mauro *et al.*, 1994, 1996; Chengalvala *et al.*, 2001). In vivo data concerning the bone-specific roles of PTPs in whole animals is more limited. Mice lacking SHP-1 are osteopenic because of increased osteoclast function (Aoki *et al.*, 1999; Umeda *et al.*, 1999), indicating that this PTP is a negative regulator of osteoclasts in vivo. To date no PTP has been shown to be a positive regulator of osteoclast activity in vivo. Better characterization of PTP function in bone can improve our understanding of regulation of bone metabolism in general and may suggest new therapeutic approaches to fight bone disease.

In this study we examine bone metabolism in mice genetically lacking PTPε. We show that cyt-PTPε is strongly expressed in osteoclasts and that young female mice genetically lacking PTPε exhibit increased trabecular bone mass; this phenotype is caused by reduced bone resorption by osteoclasts, which function abnormally both in vitro and in vivo. Reduced bone resorption is most readily detected in young (<12 weeks) female mice but markedly less so in adult female or in male mice, suggesting that lack of PTPε may affect sex hormone–related signaling pathways in osteoclasts from affected mice. At the cellular level, cultures of osteoclast-like cells from PTPε-deficient mice contain very few mature, polarized cells. These cells also exhibit abnormalities in the structure and localization of podosomes, the actin-rich adhesion structures that are necessary for proper attachment of osteoclasts to matrix and associated signaling and for subsequent bone resorption. Src activity, Pyk2 phosphorylation, and response to RANKL treatment are normal in osteoclasts from female mice lacking PTPε, suggesting these signaling pathways are not affected in a widespread manner. These results establish that PTPε is required for optimal structure and organization of podosomes in osteoclasts during cell polarization and for the optimal function of these cells in vitro and in vivo.

MATERIALS AND METHODS

Antibodies

Antibodies used in this study included polyclonal anti-PTPε (Elson and Leder, 1995a), monoclonal anti v-Src (Calbiochem, San Diego, CA), monoclonal antivinculin (clone hVin-1, Sigma, St. Louis, MO), monoclonal anti α-actinin (clone BM-75.2, Sigma), and polyclonal anti-human Pyk2 and anti-pY402 Pyk2 antibodies (Cell Signaling Technology, Beverly, MA). Horseradish peroxidase-conjugated secondary antibodies for protein blotting were purchased from Jackson ImmunoResearch Laboratories (West Grove, PA).

Mice

Gene-targeted mice lacking PTPε (*Ptpre*−/− mice, C57BL/6×129 genetic background; Peretz *et al.*, 2000) were handled in accordance with NRC regulations (NRC, 1996), Israeli law, and Weizmann Institute regulations. Numbers of mice used in each experiment are noted in the relevant figure and table legends.

Histologic Preparation and Bone Histomorphometry

This technique was performed as described (Aoki *et al.*, 1999). Briefly, tibiae were fixed in 3.7% formaldehyde, dehydrated, and embedded in methyl methacrylate resin. Sagittal sections (5 μm) were deplasticized and stained with 1% toluidine blue/1% sodium borate (Sigma). Histomorphometric parameters (Parfitt *et al.*, 1987) were measured in a 1.84 mm^2 area of secondary spongiosa starting 0.3 mm from the proximal growth plate, using the Osteomeasure analysis system (Osteometrics, Atlanta, GA).

Osteoblasts and Osteoclast-like Cells

Osteoblasts were isolated from calvariae of 1-d-old mice by sequential digestions in 0.1% collagenase (Sigma)/0.2% dispase (Roche Applied Diagnostics, Mannheim, Germany) in alpha-MEM (Sigma). Cells were grown in alpha-MEM supplemented with 10% fetal calf serum (Life Technologies-Life Sciences, Rockville, MD), 4 mM glutamine, 50 U/ml penicillin G, and 50 μg/ml streptomycin. For preparation of osteoclast-like cells (OCLs), 30–40 × 10^6 bone marrow cells were seeded per 9-cm culture dish previously seeded with 1–1.5 × 10^6 osteoblasts per dish. Cells were grown in alpha-MEM medium supplemented as above containing 10^{-8}M 1,25-dihydroxy vitamin D3 (Sigma) and 10^{-6}M prostaglandin E_2 (Sigma). Medium was changed every 2 d. After 6–8 d osteoblasts were removed by gentle flushing with medium, leaving the more adherent OCLs behind. OCLs were stained for tartarate-resistant acid phosphatase (TRAP) using a leukocyte acid phosphatase kit (Sigma). OCL nuclei were made visible by addition of 0.05% Hoechst 33342 to growth medium. WT and *Ptpre*−/− samples were always processed together.

Pit Resorption Assay

This assay was performed as described (Miyazaki *et al.*, 2003). Briefly, osteoblasts and bone marrow cells were cocultured in plates coated with rat tail collagen matrix (Roche Applied Diagnostics). Six days later collagen was removed by gentle digestion with 0.1% collagenase, and cells were seeded onto sterile dentine slices in 96-well plates. Twenty-four hours later slices were removed, immersed in 0.03N NaOCl for 5 min, sonicated for 10 s, stained for 4 min with 1% toluidine blue/1% sodium borate (Sigma), and briefly washed in water. Some pit assays were performed for 48 h in the presence of 100 ng/ml RANK ligand (Peprotech, Rocky Hill, NJ). Pit area was quantified with the Osteomeasure analysis system and was normalized to the number of osteoclasts actually present in each sample, determined by counting OCLs present in an aliquot of each coculture grown separately.

Immunofluorescence Microscopy and Image Analysis

Coculture of bone marrow and osteoblasts was performed on glass coverslips in 24-well plates. After differentiation and removal of osteoblasts by digestion in 0.1% collagenase/0.2% dispase, OCLs were permeabilized and fixed in 3% paraformaldehyde + 0.5% Triton X-100 in PBS for 2 min and then further fixed for 30 min in 3% paraformaldehyde in PBS. Fixed cells were washed three times for 5 min each in PBS and stained with primary antibody for 40 min. After washing in PBS three times, for 5 min, cells were labeled with the secondary antibody or with FITC-conjugated phalloidin (Sigma) for 40 min, and washed three times for 5 min in PBS. WT and *Ptpre*−/− samples were always processed together. Immunofluorescence microscopy was carried out with the DeltaVision system (Applied Precision Inc., Issaquah, WA) on an Axiovert 125 TV inverted microscope (Zeiss, Oberkochen, Germany). Image acquisition and processing were controlled by a Silicon Graphics workstation model O2 (Mountain View, CA) using the Resolve3D and Priism software packages (Applied Precision Inc.).

Fluorescence images were high pass filtered, and filtered images were used to produce pixel-by-pixel ratios as previously described (Zamir *et al.*, 1999). Images were arranged for publication using Adobe Photoshop v5.0.2ME (Adobe Systems Inc., San Jose, CA).

Cell Lysis, Protein Blotting, and Src Assays

Osteoblasts or OCLs (following removal of osteoblasts) were lysed in Buffer A (50 mM Tris-Cl, pH 7.5; 100 mM NaCl; 1% NP-40), containing 0.5 mM sodium pervanadate and protease inhibitors (1 mM AEBSF, 40 μM bestatin, 15 μM E-64, 20 μM leupeptin, 15 μM pepstatin; Sigma). SDS-PAGE and protein blotting was done as described (Gil-Henn *et al.*, 2001), except for Pyk2 and pY402 Pyk antibodies, where blotting was performed as per manufacturer's instructions (Cell Signaling Technology). Src was precipitated from 1 mg OCL lysates using anti–v-Src antibodies. Activity was measured in 25 μl kinase buffer (20 mM MOPS, pH 7.0, 5 mM $MgCl_2$), to which beads containing precipitated Src, 1 μl (=5 μCi) of [γ-^{32}P]ATP (3000 Ci/mmol, 10 mCi/ml, Amersham, Piscataway, NJ), and 5 μg acid-denatured enolase (Sigma) were added. Tubes were incubated at 30°C for 20 min, during which Src activity was linear with time. Samples were then electrophoresed and blotted onto membranes. Radioactivity present in enolase was quantified with a phosphorimager (BAS 2500, Fuji, Tokyo, Japan). The same blots were then probed with anti-Src antibodies and scanned with a scanning densitometer; Src activity was normalized to the amount of Src present in the immune-precipitates.

Determination of Serum Collagen Telopeptide, Estrogen, and Progesterone

Serum was prepared from blood collected by retro-orbital bleeding. Concentrations of C-telopeptide degradation products of type-I collagen in serum of 6–8-week-old mice were determined using the RatLaps ELISA system (Osteometer BioTech A/S, Herlev, Denmark). Serum estrogen and progesterone were determined using the Third Generation Estradiol and Progesterone radioimmunoassay kits, respectively (Diagnostic Systems Laboratories, Inc., Webster, TX). Serum for these hormone determinations was collected from

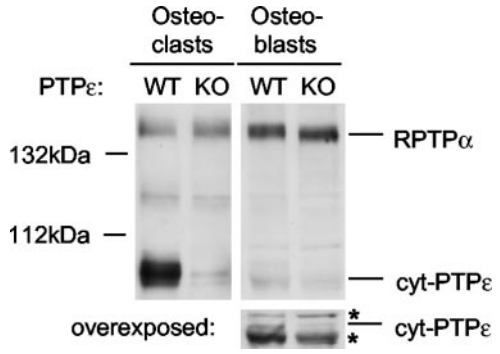

Figure 1. cyt-PTPϵ is expressed in osteoclasts. Top: Blots of protein lysates from in vitro–differentiated osteoclasts of 6-week-old mice and from calvarial osteoblasts were probed with anti-PTPϵ antibodies. Note high expression of cyt-PTPϵ in WT, but not *Ptpre−/−*, osteoclasts and very low expression in osteoblasts. Bottom: strong overexposure of bottom portion of osteoblast blot; arrow marks cyt-PTPϵ, asterisks mark non-PTPϵ bands. Antibody used cross-reacts also with RPTPα (Elson and Leder, 1995a); identity of indicated band was confirmed separately by blotting with a second, RPTPα-specific antibody. RPTPα is easily detected in osteoclasts, but is more strongly expressed in osteoblasts.

4-week-old female mice weaned 1 week previously and from 12-week-old female mice.

RESULTS

Osteoclasts Express High Levels of the Nonreceptor Form of PTPϵ

The connection between PTPϵ and Src activation and between Src activity and bone structure prompted us to examine bone homeostasis in mice genetically lacking PTPϵ. Expression of PTPϵ protein was examined in calvarial osteoblasts and in OCLs, which were produced using the bone-marrow/osteoblast coculture technique and purified by removal of osteoblasts before analysis. Osteoblasts and OCLs were derived from wild-type mice and from mice genetically lacking PTPϵ (*Ptpre−/−* mice), which lack all four known forms of PTPϵ protein (Peretz *et al.*, 2000). Blotting experiments indicated that the nonreceptor form of PTPϵ (cyt-PTPϵ; Elson and Leder, 1995b, Nakamura et al., 1996) appears to be strongly expressed in OCLs of wild-type, but not in *Ptpre−/−* OCLs (Figure 1). In contrast, very weak expression of cyt-PTPϵ was detected in osteoblasts. OCLs from WT mice expressed similar levels of cyt-PTPϵ protein in a manner independent on mouse age (5–8 vs. 20–24 weeks) or gender (unpublished results). In contrast with PTPϵ, the closely related RPTPα was detected in OCLs and at higher levels in osteoblasts. Expression of RPTPα was not increased in *Ptpre−/−* cells to compensate for loss of PTPϵ (Figure 1). The protein expression patterns of both PTPs agree with those determined by mRNA analysis (Schmidt *et al.*, 1996), although we show here that the form of PTPϵ protein expressed in OCLs appears to be the nonreceptor form of the phosphatase. This finding agrees with detection of cyt-PTPϵ mRNA and protein in spleen, lymph nodes, macrophages, and in hematopoietic cells induced to differentiate along the monocyte-macrophage pathway, from which osteoclasts are derived (Elson and Leder, 1995b; Tanuma *et al.*, 1999; Sully *et al.*, 2001).

Young Female Ptpre−/− Mice Display Increased Bone Mass Due to Impaired Osteoclast Function

To determine whether lack of PTPϵ is associated with abnormal bone structure in vivo, we performed histomorphometric analyses on tibiae of WT and *Ptpre−/−* mice. Analyses included male and female mice, aged 2 weeks, 7 weeks, and 3 months. As shown in Table 1, in which data from mice aged 7 weeks is presented, trabecular bone volume was increased by 109% and the number of trabeculae was increased by 68% in *Ptpre−/−* female mice. Strong tendencies, on the verge of statistical significance, were also noted in trabecular thickness (28% increase) and trabecular separation (38% decrease). A slight (5.6%) but statistically significant ($p = 0.025$) increase in *Ptpre−/−* tibial length was also noted (unpublished results). Increases in trabecular number were also detected by direct histological staining of bone samples (Figure 2A). Trabecular bone volume is then increased in *Ptpre−/−* female mice, but not in age-matched male mice. Similar results were obtained when samples

Table 1. Histomorphometric analyses of the cancellous region of the tibial metaphysis of 7 week-old female and male mice[a]

	Bone mass				Bone formation			Bone degradation	
	BV/TV (%)	Tb.Th (μm)	Tb.N (/mm)	Tb.Sp (mm)	OV/TV (%)	Ob.S/BS (%)	MAR	N.Oc/BS (/mm)	Oc.S/BS (%)
Females									
KO	6.92 ± 1.02	20.27 ± 1.76	3.38 ± 0.32	298.3 ± 43.8	8.59 ± 1.64	34.68 ± 2.36	1.19 ± 0.08	1.09 ± 0.25	3.77 ± 0.90
WT	3.31 ± 0.44	15.85 ± 0.95	2.01 ± 0.20	478.3 ± 83.5	6.59 ± 1.77	25.96 ± 6.21	1.24 ± 0.10	3.45 ± 0.63	9.44 ± 1.74
p value	0.01 (+109%)[b]	0.06 (+28%)	0.01 (+68%)[b]	0.07 (−38%)	N	N	N	<0.001 (−69%)[b]	0.01 (−60%)[b]
Males									
KO	5.84 ± 1.23	18.30 ± 1.62	3.01 ± 0.33	331 ± 31.8	2.41 ± 0.50	20.30 ± 8.29	1.10 ± 0.07	2.40 ± 0.53	7.04 ± 1.75
WT	5.80 ± 1.13	17.31 ± 1.00	3.37 ± 0.63	362.3 ± 92.7	4.24 ± 1.33	16.48 ± 2.73	1.05 ± 0.06	1.71 ± 0.34	4.80 ± 0.92
p value	N	N	N	N	N	N	N	N	N

[a] Parameters analyzed are as follows: trabecular bone volume (% of bone volume) (BV/TV); trabecular thickness (Tb.Th); trabecular number (Tb.N); trabecular spacing (Tb.Sp); osteoid volume (% of bone volume) (OV/TV); osteoblast surface (% of bone surface) (Ob.S/BS); mineral apposition rate (MAR); number of bone-adherent osteoclasts per unit of bone surface (N.Oc/BS); osteoclast surface (% of bone surface) (Oc.S/BS). Data (mean ± SE) are from n = 5–6 mice for each genotype and gender. Unpaired, two-tailed p values are by Student's *t*-test or the Mann-Whitney test; Qualitatively similar results were obtained in analyses of similar numbers of 2-week-old female and male mice; no differences were observed when similar numbers of 3-month-old mice, males and females, were analyzed (unpublished data).

[b] Statistically significant data.

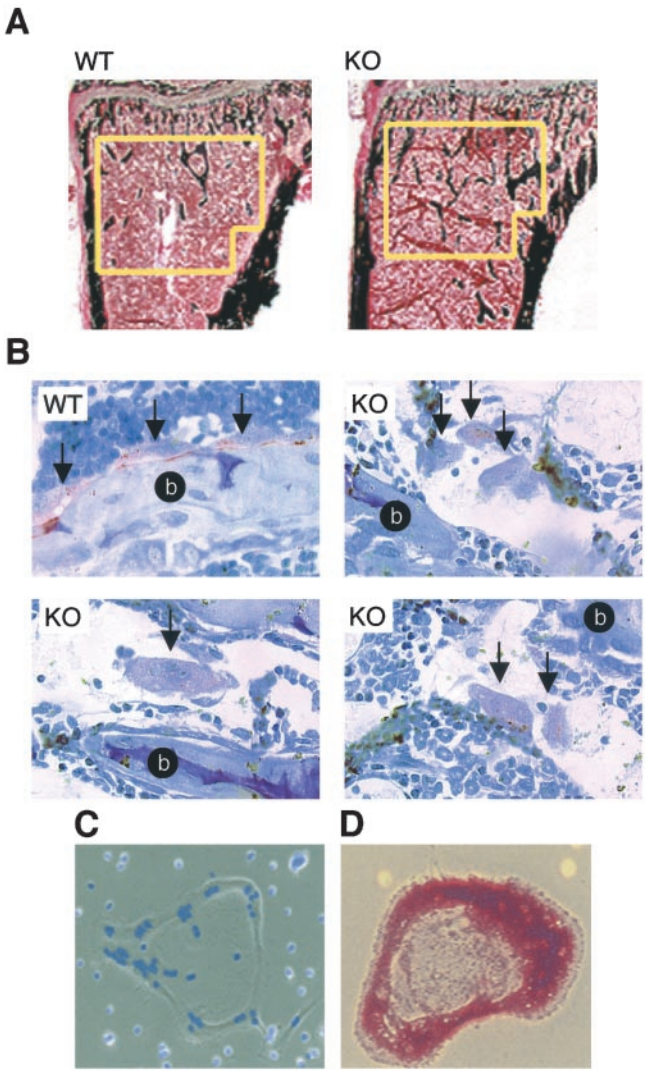

Figure 2. Histologic examination of *Ptpre−/−* tibiae and osteoclasts. (A) Cross section of tibiae from 7-week-old wild-type (WT) and *Ptpre−/−* (KO) female mice stained according to the method of von Kossa. Yellow lines highlight more prominent trabecular bone (black, within the red counterstain) in *Ptpre−/−* sample. (B) Unattached osteoclasts in *Ptpre−/−* bone. Shown are histological analyses of bone samples from 7-week-old wild-type and *Ptpre−/−* mice stained for tartarate-resistant acid phosphatase (TRAP) activity (red-purple, a marker of osteoclasts) and counterstained with toluidine blue (blue). OCLs (attached to bone in WT samples, unattached in KO samples) are indicated by arrows; bone matrix is indicated by a lowercase b on black background. (C) Multinucleated PTPε-deficient osteoclast-like cell (OCL; light microscopy, gray) stained with Hoechst 33342 to highlight nuclei (blue). Original magnification, ×100. (D) PTPε-deficient OCL, stained for TRAP (red). Light microscopy, original magnification, ×20. Data in C and D were obtained from 7-week-old mice; similar data were obtained from OCLs of wild-type mice.

from similar numbers of male and female mice of both genotypes aged 2 weeks were analyzed (unpublished results). Differences in bone volume were not detected in mice of either gender at 3 months of age (unpublished results), indicating that the bone phenotype of young female mice is abrogated at a time roughly coinciding with these mice reaching full sexual maturity. No changes in bone structure

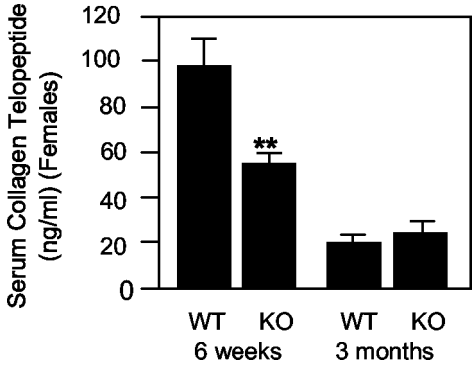

Figure 3. Serum collagen telopeptide concentrations are reduced in young *Ptpre−/−* female mice. Collagen telopeptide concentrations (mean ± SE) were determined in serum by radioimmunoassay in female mice, aged 6 weeks and 3 months. **p = 0.03 by Student's *t* test. n = 5 mice per genotype and age group. Experiment is representative of three performed, for a total of 15 mice per genotype and age group. Note the normal reduction in telopeptide concentrations as mice age.

were revealed upon examination of calvarial membranous bones of 2-week-old *Ptpre−/−* mice, which expressed the trabecular bone phenotype.

Histomorphometric analyses also indicated that young female *Ptpre−/−* mice synthesize bone normally, but have significant defects in bone resorption. Bone formation parameters, such as osteoid volume, osteoblast surface, and mineral apposition rate were not changed in *Ptpre−/−* mice (Table 1). In contrast, *Ptpre−/−* female mice exhibited a 69% reduction in the number of osteoclasts in contact with bone and a corresponding 60% reduction in bone surface in contact with osteoclasts (Table 1). It should be noted that a normal number of osteoclasts was detected in samples from *Ptpre−/−* female mice. However, a large fraction of these cells were not in contact with bone (shown qualitatively in Figure 2B), possibly indicating difficulties in adhesion of *Ptpre−/−* osteoclasts to bone matrix in vivo. This abnormality was observed only in young *Ptpre−/−* female mice and coincided with increased bone volume determined by histomorphometry in these mice (Table 1). In all, these data indicate that the defect in bone degradation is due to abnormal functioning of osteoclasts rather than to a reduction in their numbers. Osteoblasts appear not to be affected in *Ptpre−/−* mice, in agreement with the very low levels of cyt-PTPε expression in these cells.

Further support for an osteoclast-related defect in young *Ptpre−/−* female mice was obtained when serum levels of C-terminal collagen telopeptide, a specific product of bone degradation by osteoclasts in vivo, were determined. Female *Ptpre−/−* mice aged 6 weeks exhibited a 44% reduction in serum collagen telopeptide concentrations (Figure 3). In contrast, collagen telopeptide concentrations in age-matched *Ptpre−/−* male mice and in older *Ptpre−/−* female mice, which were normal by histomorphometric analysis, were similar to those of matched wild-type control mice (Figure 3 and unpublished results).

PTPε-deficient Osteoclasts Are Inherently Defective

Results presented thus far indicate that *Ptpre−/−* mice suffer from a defect in osteoclast function. To examine whether *Ptpre−/−* osteoclasts are inherently defective, we examined the formation and function of OCLs in vitro. This study used the bone marrow/osteoblast coculture system, in which

bone marrow cells are cocultured with calvarial osteoblasts allowing marrow-derived osteoclast precursor cells to differentiate into OCLs. Osteoblasts of either genotype induced bone marrow differentiation to similar extents, and bone marrow cells from either genotype produced similar amounts of OCLs (unpublished results). *Ptpre*−/−and WT OCLs exhibited features typical of osteoclasts in general such as large size, flat morphology, multinucleation, and intense staining for TRAP (Figure 2, C and D). Cultures of WT and or *Ptpre*−/− OCLs appeared generally similar when examined by light microscopy. However, more detailed examination by immunofluorescence microscopy revealed disruptions in the actin-rich podosome array at periphery of *Ptpre*−/− OCLs, as is described further below.

To determine whether *Ptpre*−/− OCLs were functional, OCLs produced in vitro were seeded onto dentine slices and allowed to excavate pits in the dentine matrix. Twenty-four hours later the cells were removed and the pits were stained and quantified. As seen in Figure 4A, the area of pits excavated by *Ptpre*−/− OCLs prepared from young (7–8 weeks old) female mice was significantly reduced when compared with WT OCLs. *Ptpre*−/− OCLs from age-matched male mice exhibited a reproducible trend for reduced pit area, but this did not reach statistical significance. Pits formed by *Ptpre*−/− OCLs from young female mice were also strikingly shallower, as indicated by the extent of their staining (Figure 4B). A slight, although not significant, trend for reduced resorption was detected in OCLs from older (15 weeks old) *Ptpre*−/− female mice (Figure 4C). These data indicate that OCLs derived from mice that exhibit a more severe bone phenotype in vivo are those that function least well in bone resorption assays in vitro under controlled and identical conditions, indicating that these cells are inherently defective.

Disrupted Organization of Podosomes in Ptpre−/− OCLs

To better understand the causes of reduced bone resorption in vitro by *Ptpre*−/− OCLs we examined the structural organization of these cells. Although populations of WT and *Ptpre*−/− OCLs appeared quite similar when examined by light microscopy, immunostaining revealed striking differences between OCLs of both genotypes. In particular, abnormalities were observed in *Ptpre*−/− OCLs in the organization of podosomes, the actin-rich multiprotein adhesion structures that form a ring-like array in the sealing zone, at the periphery of mature, polarized osteoclasts (Marchisio *et al.,* 1984, 1987; Tarone *et al.,* 1985; Nermut *et al.,* 1991; reviewed in Linder and Aepfelbacher, 2003). Staining OCLs for the podosomal proteins actin or α-actinin revealed several levels of organization of podosomes in these cells, which reflect the various states of polarization found in the OCL population (Figure 5A). Accordingly, 42.5 ± 2.6% (mean ± SE) of WT OCLs contained podosomes that were all distributed in an apparently random manner, indicating that these cells were not polarized. In 35.5 ± 2.6% of cells podosomes were evenly distributed in a circular array at the cell periphery, as is seen in fully mature, polarized OCLs. In the remaining 22 ± 2.0% of WT OCLs podosomes were found in intermediate levels of arrangement (Figure 5A). In stark contrast, the *Ptpre*−/− OCL population exhibited significantly more cells with random arrangement of podosomes (69.3 ± 3.5%) and a 10-fold drop (to 3.2 ± 1.4%) in polarized cells that displayed a full podosomal array at the cell periphery. OCLs displaying intermediate levels of podosome organization were as prevalent in *Ptpre*−/− samples (27.5 ± 3.2%) as they were in WT samples (Figure 5A).

Further close examination revealed qualitative differences between the appearance of actin arrays in WT vs. *Ptpre*−/− OCLs. The podosome arrays at the periphery of polarized WT OCLs contained individual, evenly distributed podosomes that were surrounded by a diffuse actin "cloud" (Figure 5, B, D, and F; Destaing *et al.,* 2003). In contrast, significant irregularities were observed even in the rare *Ptpre*−/− OCLs that displayed what appeared at low magnification to be fully formed podosomal arrays at the cell periphery (e.g., Figure 5C). Actin arrays in such cells contained many large clusters of podosomes next to array regions that contained no clusters and few individual podosomes (Figures 5, E, G, and H). Many of these podosome-poor regions also contained actin structures of ill-defined morphology (Figure 5, E and H); the diffuse actin cloud that normally surrounds individual podosomes in WT OCLs was not detected. Interestingly, the above differences were limited to podosome arrays at the periphery of OCLs. No differences were detected between nonpolarized WT and *Ptpre*−/− OCLs, and cells from both genotypes contained individual podosomes arranged in an apparently random manner. In partially polarized OCLs, which contained podosome arrays as well as regions of podosomes arranged at random, differences between the genotypes were limited to the podosome arrays (unpublished results).

Disorganization of the podosome arrays was evident also when the distribution of other podosome-associated structural proteins was examined. For example, vinculin, which is located in the protein ring that surrounds the actin core of podosomes (Linder and Aepfelbacher, 2003), was detected around the individual evenly spaced actin-rich podosome cores of WT OCLs (Figures 6, C and G). In contrast, the uneven distribution of podosome cores in *Ptpre*−/− OCLs created large regions of strong contiguous actin staining, some devoid of vinculin and others surrounded by abnormally shaped vinculin rings (Figure 6, F and H). In addition, actin cores not surrounded by vinculin rings were often observed in *Ptpre*−/− OCLs at the sealing zone, as were uneven protrusions of vinculin from the podosome array region toward the cell periphery (Figures 6, F and I). Together, these findings suggest that lack of PTPε adversely affects the structure of individual podosomes, the organization of podosome arrays within OCLs, and the amount of polarized OCLs, in correlation with the reduced abilities of these cells to resorb bone in vitro.

Total Src Activity and Pyk2 Phosphorylation Are Not Affected in Ptpre−/− OCLs

Mice lacking Src are osteopetrotic because of reduced osteoclast function. Because PTPε activates Src in fibroblasts and absence of PTPε reduces Src activity in mammary tumor cells (Gil-Henn and Elson, 2003), we asked whether the *Ptpre*−/− bone phenotype was associated with reduced Src activity in OCLs. Measurements performed in lysates of OCLs revealed similar levels of Src kinase activity in OCLs of *Ptpre*−/− and WT mice of either gender or age (Figure 7A), arguing against the *Ptpre*−/− bone phenotype being mediated by widespread changes in Src activity. Phosphorylation of Pyk2 at Y402, an autophosphorylation site that enables Pyk2 to associate with Src (Duong *et al.,* 1998; Sanjay *et al.,* 2001; Lakkakorpi *et al.,* 2003), was also unchanged in OCL lysates (Figure 7B). We conclude that lack of cyt-PTPε does not cause widespread dysregulation of these signaling pathways, although this does not entirely preclude existence of more limited and localized changes in these pathways. Interestingly, resorption by OCLs from young or older females of both genotypes was increased in the presence of

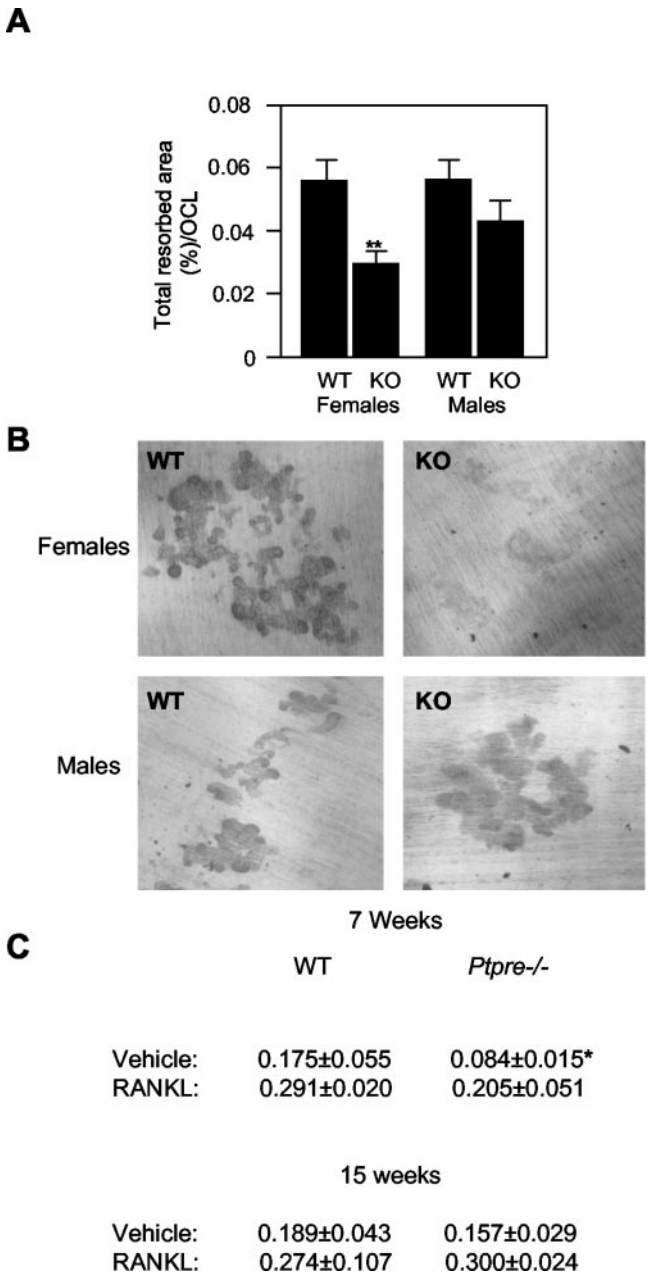

Figure 4. Reduced bone-resorbing activity of OCLs from young female mice lacking PTPε. in vitro–differentiated OCLs of WT or *Ptpre*−/− (KO) mice, males and females aged 8 weeks (n = 3 per genotype and gender), were seeded onto dentine slices and incubated for 24 h. Cells were then removed, and pits were stained with toluidine blue. (A) Area of pits excavated by OCLs, normalized to total number of OCLs present, as a fraction of total dentine surface area. Data (mean ± SE) are from three experiments. **p = 0.0059 by the Mann-Whitney test. (B) Light microscopy images of pits excavated by WT or *Ptpre*−/− OCLs from female (top) and male (bottom) mice in one of the experiments summarized in A. OCLs from *Ptpre*−/− female mice excavate pits of smaller area (A) as well as of significantly reduced depth (reduced staining in B). (C) Pit resorption assay performed in young (7 weeks) vs. older (15 weeks) female mice, in the absence or presence of 100 ng/ml RANKL. Shown is area of pits excavated, normalized to number of OCLs present, as a fraction of total dentine surface area. n = 3 for each sample; *p < 0.05 by Student's *t* test, vs. WT of same age. Note that OCLs from older female *Ptpre*−/− mice resorb dentine normally and that OCLs from young or older *Ptpre*−/− mice respond to RANKL treatment. Bone resorption was allowed to proceed for 48 h (vs. 24 h in A).

RANK ligand (RANKL; Figure 4C), a strong stimulator of OCL activity. This indicates that this major signaling pathway is functional in *Ptpre*−/− OCLs, and agrees with normal production of *Ptpre*−/− OCLs, in which RANKL signaling is important.

Detection of the above phenotype in young female mice and its disappearance as mice reach full sexual maturity suggests that other factors, perhaps concentrations of systemic hormones, influence the phenotype as well. Measurements of estrogen, a key hormone that regulates bone mass, in sera of 4-week-old female mice revealed similar levels in WT and in *Ptpre*−/− mice (values presented as mean ± SE: WT: 16.46 ± 1.00 pg/ml, n = 13; *Ptpre*−/−: 15.22 ± 0.48 pg/ml, n = 16; p = 0.249 by Student's *t* test). Estrogen levels in sera of 12-week-old female WT and *Ptpre*−/− mice were similar as well. Serum levels of another major sex hormone, progesterone, were also similar in 4-week-old WT and *Ptpre*−/− females (mean ± SE: WT: 0.99 ± 0.15 ng/ml, n = 15; *Ptpre*−/−: 0.91 ± 0.11 ng/ml, n = 16; p = 0.672 by Student's *t* test). Concentrations of testosterone, which is also known to impact OCL function, in sera of male *Ptpre*−/− and WT mice were also similar; levels of this hormone were below detection in sera of female mice (unpublished results). We conclude that altered concentrations of these hormones are not the cause of the bone phenotype found in young female *Ptpre*−/− mice.

DISCUSSION

This study demonstrates that lack of PTPε can lead to a gain in bone mass, which is due to reduced function of osteoclasts. Several experimental results converge to support this conclusion. These include detection of increased trabecular bone volume in *Ptpre*−/− mice by several independent histomorphometric parameters and by histologic examination, reduced serum concentrations of collagen degradation fragments, which are osteoclast-specific products of bone resorption in vivo, and poor function of *Ptpre*−/− OCLs in in vitro functional assays. We conclude that the normal physiological role of PTPε in osteoclasts is to support the bone-resorbing activity of these cells in vivo. Because osteoclasts and macrophages are products of the same hematopoietic developmental pathway, this conclusion is consistent also with existence of functional abnormalities in PTPε-deficient macrophages (Sully *et al.*, 2001). Of note, the bone phenotype of *Ptpre*−/− female mice is less severe than, for example, Src-deficient mice, indicating that the *Ptpre*−/− osteoclast population is partially functional despite lack of PTPε.

Abnormalities in podosome organization in *Ptpre*−/− OCLs that have been described here allow us to further refine our understanding of the role cyt-PTPε fulfills in osteoclasts. Osteoclasts alternate between periods of resorption, when they adhere tightly to matrix, and migration, when tight association with the matrix must be relaxed. Organization of podosomes, the primary cellular structure by which osteoclasts adhere to matrix (Marchisio *et al.*, 1984, 1987; Tarone *et al.*, 1985; Zambonin-Zallone, 1988; Nermut *et al.*, 1991), is therefore critical in this respect. Podosomal arrays at the cell periphery are found in actively resorbing, polarized osteoclasts, whereas podosomes in migrating osteoclasts are less ordered (Lakkakorpi and Vaananen, 1991). In agreement with the changing nature of cell-matrix adhesion in osteoclasts and with its regulation by extracellular signals (Sanjay *et al.*, 2001), podosomes are very dynamic structures and their major protein components undergo turnover within minutes (Stickel and Wang, 1987; Chen,

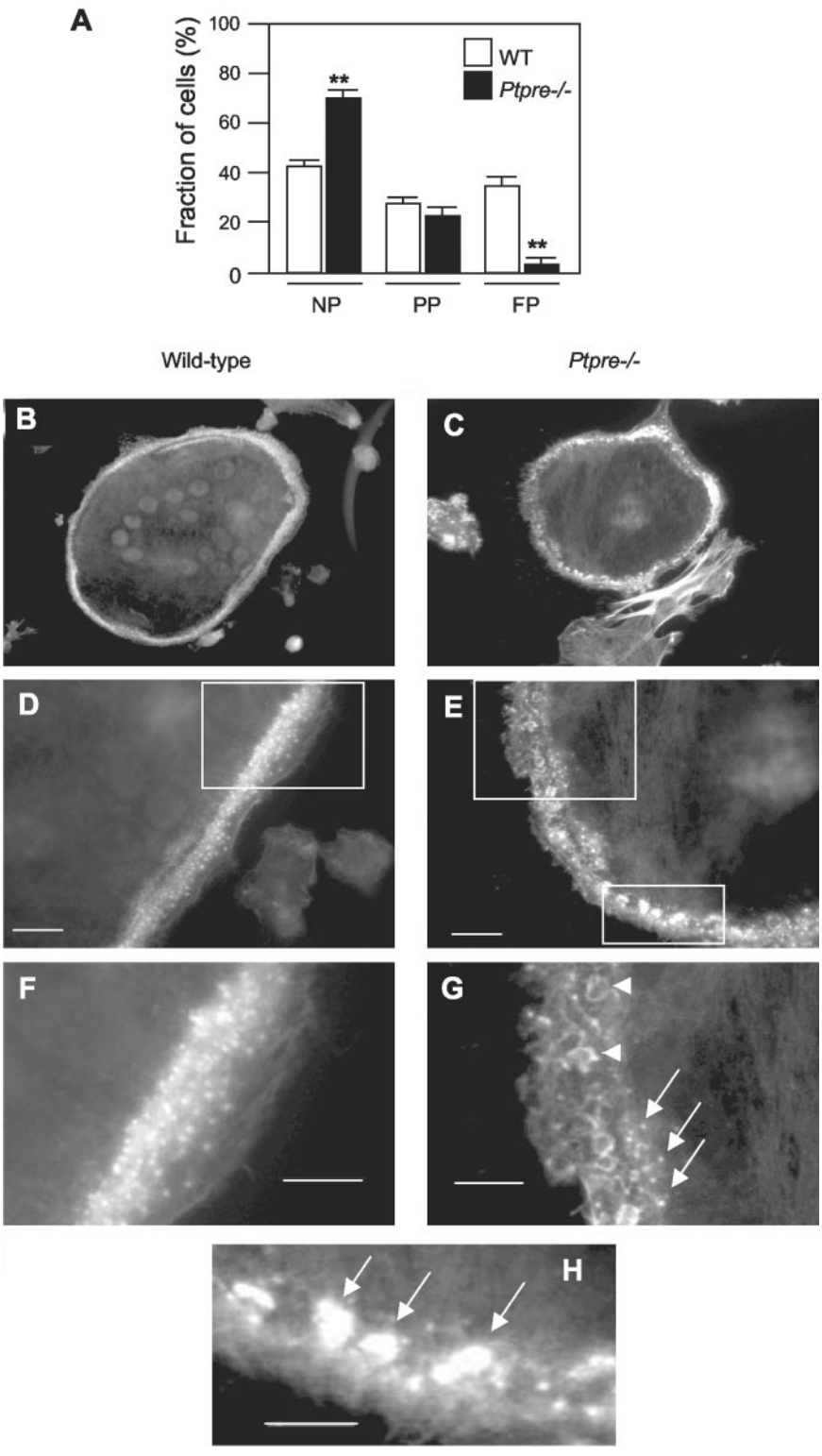

Figure 5. Disorganization of podosomes in *Ptpre*−/− OCLs. (A) OCLs from 4-week-old WT and *Ptpre*−/− female mice were stained for α-actinin to reveal podosome organization. Cells in independent fields were classified as nonpolarized (NP, podosomes spread throughout cell randomly), partially polarized (PP, podosomes in part of the cell arranged in an array or array-like manner), or fully polarized (FP, podosomes arranged in an array at the cell periphery). Histogram shows percentage of cells in each morphological class in both genotypes and summarizes data from a total of 213 WT OCLs (31 fields) and 224 *Ptpre*−/− OCLS (29 fields) examined in two independent experiments. $^{**}p < 0.0001$ by the Mann-Whitney test. Qualitatively similar results were obtained when cells were stained for actin. (B–H) Disorganization of podosomes in *Ptpre*−/− OCLs. WT and a *Ptpre*−/− OCLs were stained for actin and are shown at ×40 (B and C) and at ×100 (D and E) magnification. Higher power magnifications of regions marked by rectangles in D and E are shown in F–H. Note individual podosomes on the background of the actin "cloud" in the WT cell (F). In contrast, *Ptpre*−/− OCLs contain regions of few individual podosomes (arrows, G) and regions containing ill-defined actin-rich structures (arrowheads, G). Same cell also contains clusters of podosomes (arrows, H). Bars, (D and E) 10 μm; (F–H) 5 μm.

1989; Destaing *et al.*, 2003; Evans *et al.*, 2003). Abnormalities in podosomal organization would then be expected to affect migration, adhesion, and bone resorption by OCLs. It is therefore tempting to speculate that functional abnormalities in *Ptpre*−/− osteoclasts, manifested as nonadherent osteoclasts in vivo and reduced bone resorption by osteoclasts in vivo and by OCLs in vitro, result from podosome disorganization.

Interestingly, podosome disorganization in *Ptpre*−/− OCLs affected podosomal arrays, which are characteristic of osteoclasts that are able to resorb bone or that are preparing to do so. cyt-PTPε then appears to be required when podo-

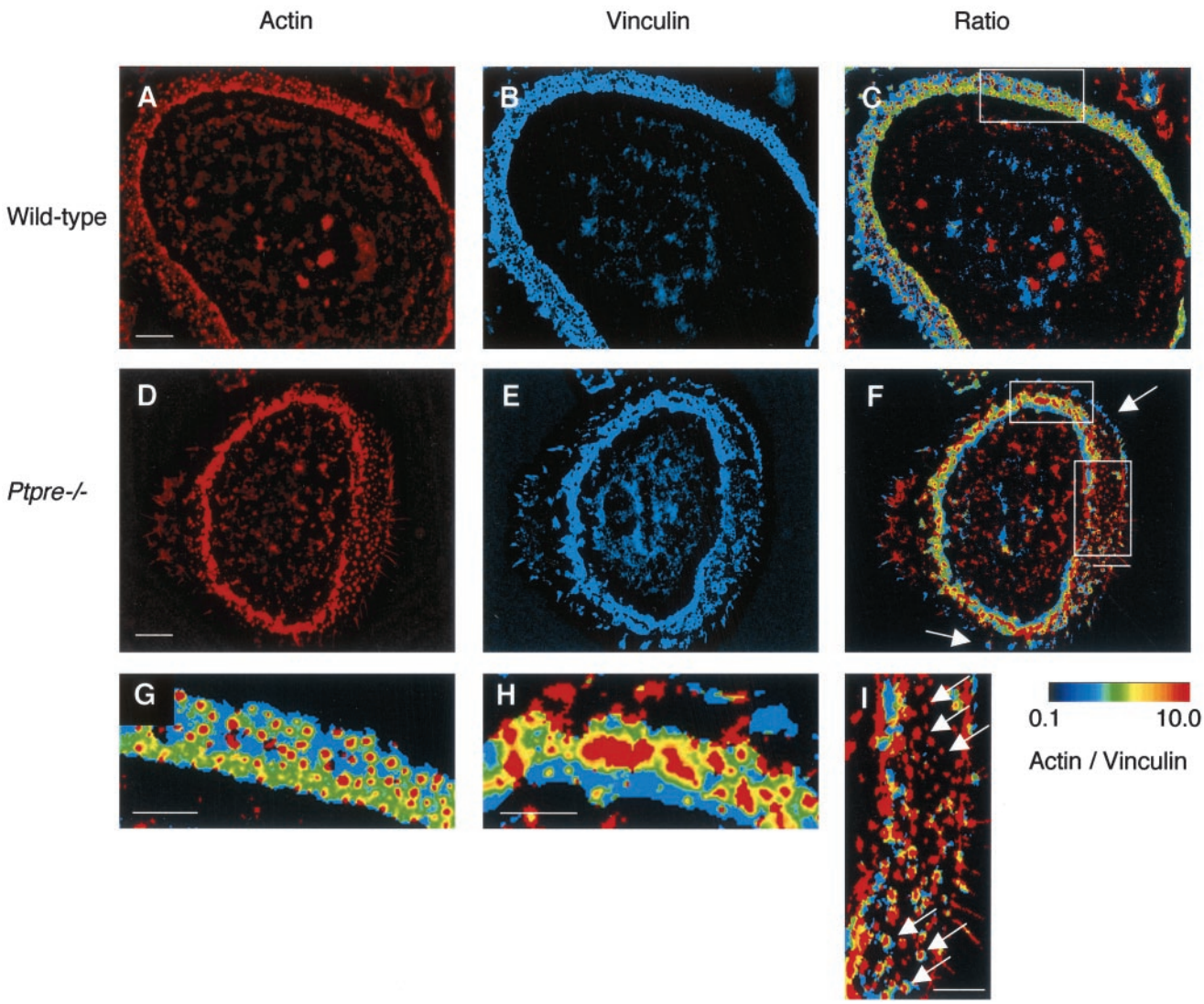

Figure 6. Vinculin is disorganized in *Ptpre*−/− podosomes. Double immunostaining for actin (A and D, WT and *Ptpre*−/−, respectively) and vinculin (B and E). (C and F) A combination of actin and vinculin fluorescence. WT (G) and *Ptpre*−/− (H and I) show higher-powered magnifications of areas within rectangles in C and F. Colors in C, F, G, H, and I represent the ratio between actin and vinculin staining intensities (Zamir *et al.*, 1999), according to the scale to the right of I; warmer colors indicate more actin relative to vinculin. Note individual actin cores surrounded by vinculin in WT samples (G) vs. multiple clustered podosome cores that contain little or no vinculin in *Ptpre*−/− OCLs (H). *Ptpre*−/− OCLs contain concentrations of vinculin that extend distally without accompanying actin (arrows in F). Also seen in *Ptpre*−/− OCLs are actin cores of podosomes devoid of surrounding vinculin (top arrows in I; compare with lower arrows in same panel, which show cores surrounded by minute "rosettes" of vinculin). Note that size of actin cores in this region is comparable to WT podosome cores. Cell shown in D–F, H, and I is among the best-organized *Ptpre*−/− OCLs. Bars, (A and D) 10 μm; (G–I) 5 μm.

somes are arranged into the peripheral array during the process of polarization in preparation for bone resorption. Interactions between individual podosomes have been suggested to exist, with podosomes being formed in the vicinity of previously existing podosome groups (Destaing *et al.*, 2003). Podosomes have also been suggested to undergo cycles of fusion and fission, and large aggregates, termed podosome cluster precursors (PCPs), that can fragment into individual podosomes have recently been described in macrophages (Evans *et al.*, 2003). Detection of large clusters of actin-rich structures within the peripheral array of *Ptpre*−/− OCLs (Figure 5) may suggest that cyt-PTPε is required to maintain proper balance between large podosomal clusters vs. individual podosomes.

The transient nature of the bone phenotype is intriguing. In particular, disappearance of the bone phenotype in female *Ptpre*−/− mice at an age that roughly coincides with their reaching full sexual maturity and absence of a significant bone phenotype in male *Ptpre*−/− mice suggest that the intrinsic defect in *Ptpre*−/− osteoclasts is modulated by systemic effects of sex hormones. These effects could be mediated by alterations in levels of specific hormones in *Ptpre*−/− female mice or by aberrant responses of osteoclast precursors in these mice to normal hormone levels. Our data do not support the first possibility because serum levels of the major sex hormones estrogen and progesterone in younger and in older *Ptpre*−/− mice are similar to those measured in WT controls. On the other hand, significant

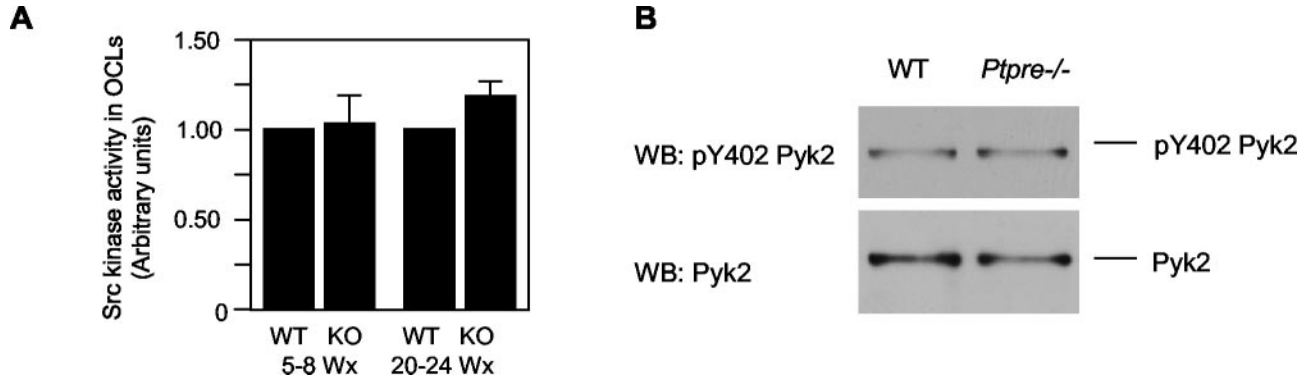

Figure 7. (A) Src activity is not altered in young (5–8 weeks) or in older (20–24 weeks) *Ptpre*−/− female mice. Shown is Src activity (mean ± SE) in extracts of OCLs prepared from *Ptpre*−/− female mice relative to that of matched WT mice. Differences between groups were not statistically significant ($p > 0.05$, Student's *t* test; n = 13 (young), n = 7 (older) mice per genotype and age group). Similar results were obtained with male mice (unpublished results). (B) Autophosphorylation of Pyk2 at Y402 is unchanged in whole cell lysates of OCLs prepared from young female WT and *Ptpre*−/− mice. Lysates were blotted and probed with anti pY402 Pyk2 antibodies; membranes were then stripped and reprobed with phospho-insensitive anti-Pyk2 antibodies. Similar results were obtained in OCLs from older female mice (unpublished data).

support for an osteoclast-specific defect in *Ptpre*−/− mice comes from the finding that bone resorption in vitro is abnormal in OCLs of young *Ptpre*−/− female mice, but appears normal in OCLs from male or older female mice (Figure 4). This result is significant because OCLs were grown and assayed in these experiments under defined and identical conditions for all samples. Detection of abnormalities only in OCLs from young female *Ptpre*−/− mice then indicates that these cells are inherently abnormal. One can then speculate that as female mice mature, changing levels of estrogen or of other hormones may induce compensatory mechanisms in OCL precursors, which abrogate the bone phenotype of *Ptpre*−/− female mice. Because cyt-PTPε protein levels are not changed in OCLs from mature mice, examples of such mechanisms may include induction of another PTP that can perform the functions of PTPε or reduced need for these functions. Of note, protein levels of the highly related RPTPα are not changed in OCLs as mice mature (unpublished results). This proposed mechanism could account for the gender- and age-specific aspects of the *Ptpre*−/− bone phenotype, although its molecular basis is complex and requires further study.

The response of *Ptpre*−/− OCLs to RANK ligand, a strong stimulator of bone resorption activity, is normal. This major signaling pathway is then functional despite loss of PTPε, consistent with normal production of *Ptpre*−/− osteoclasts in which RANKL signaling plays an important role. Total Src activity and phosphorylation of Y402 in Pyk2, a site required for Src-Pyk2 interactions during activation of integrin signaling in osteoclasts (Sanjay *et al.*, 2001), are also normal in lysates of OCLs from *Ptpre*−/− mice, despite the ability of cyt-PTPε to activate Src in several cell types (Gil-Henn and Elson, 2003). These results indicate that the *Ptpre*−/− bone phenotype is not due to widespread disruption of these signaling pathways. It should be noted that the bone phenotypes of *Ptpre*−/− and Src-deficient mice are not identical. This is shown, for example, by the stronger osteopetrotic phenotype of Src-deficient mice and by the relative ease with which OCLs can be cultured from bone marrow precursors of *Ptpre*−/− mice as compared with Src-deficient mice. Interestingly, Src activity is not altered also in Schwann cells from *Ptpre*−/− mice, a cell type that also normally expresses cyt-PTPε. *Ptpre*−/− Schwann cells exhibit aberrant phosphorylation and function of the integral membrane Kv2.1 and Kv1.5 potassium channels, and their myelinating abilities are transiently impaired (Peretz *et al.*, 2000). In contrast, absence of RPTPε from Neu-induced mammary tumor cells reduces Src activity and is at least partially responsible for the phenotype of these cells (Gil-Henn and Elson, 2003). Although a fraction of cyt-PTPε molecules are found at the cell membrane (Elson and Leder, 1995b; Gil-Henn *et al.*, 2000), a basic distinction may then exist between RPTPε and cyt-PTPε, with the former being more able to act through Src in vivo or being less functionally redundant with other PTPs that also target Src. It is of interest to note that OCLs express significant amounts of the highly related receptor-type PTPα (Figure 1), which can also dephosphorylate and activate Src (Zheng *et al.*, 1992; Ponniah *et al.*, 1999; Su *et al.*, 1999). Presence of RPTPα may therefore prevent changes in Src activity due to loss of the fraction of cyt-PTPε normally found at the cell membrane. Absence of cyt-PTPε from other regions of the cell may lead to the OCL and bone phenotypes by disrupting signaling in a localized manner. Examination of the bone phenotype of RPTPα-deficient mice is therefore of interest.

Bisphosphonates, antiosteoporotic drugs that disrupt osteoclast function, are believed to function by inhibition of the mevalonate pathway (Fisher *et al.*, 1999, 2000; Rogers *et al.*, 2000). However, previous studies have shown that the bisphosphonates alendronate and tiludronate inhibit the activities of several PTPs, among them PTPε, by a mechanism that may involve oxidation of their catalytic cysteine (Endo *et al.*, 1996; Schmidt *et al.*, 1996; Murakami *et al.*, 1997; Opas *et al.*, 1997; Skorey *et al.*, 1997). This raises the possibility that part of the antiosteoporotic function of these compounds may be due nonetheless to their inhibition of PTPs. Examination of bone structure in mice lacking other PTPs may help clarify this issue and provide additional information on the roles of specific tyrosine phosphatases in regulation of bone mass.

ACKNOWLEDGMENTS

We thank Prof. Benny Geiger of the Weizmann Institute for helpful advice and discussions. We also thank Judith Hermesh and her colleagues at the Weizmann Institute Transgenic Mouse Facility for expert animal care. This study was supported by a grant from the United States-Israel Binational Science Foundation to A.E. and by Grant AR42927 from the National Institutes of Health, NIAMS, to R.B. A.E. is incumbent to the Adolfo and Evelyn

Blum Career Development Chair in Cancer Research at the Weizmann Institute.

REFERENCES

Andersen, J.N., Elson, A., Lammers, R., Romer, J., Clausen, J.T., Moller, K.B., and Moller, N.P.H. (2001a). Comparative study of protein tyrosine phosphatase-epsilon isoforms: membrane localization confers specificity in cellular signalling. Biochem. J. *354,* 581–590.

Andersen, J.N. *et al.* (2001b). Structural and evolutionary relationships among protein tyrosine phosphatase domains. Mol. Cell. Biol. *21,* 7117–7136.

Aoki, K. *et al.* (1999). The tyrosine phosphatase SHP-1 is a negative regulator of osteoclastogenesis and osteoclast resorbing activity: increased resorption and osteopenia in me(v)/me(v) mutant mice. Bone *25,* 261–267.

Boyce, B.F., Yoneda, T., Lowe, C., Soriano, P., and Mundy, G.R. (1992). Requirement of pp60c-src expression for osteoclasts to form ruffled borders and resorb bone in mice. J. Clin. Invest. *90,* 1622–1627.

Chen, W.T. (1989). Proteolytic activity of specialized surface protrusions formed at rosette contact sites of transformed cells. J. Exp. Zool. *251,* 167–185.

Chengalvala, M.V., Bapat, A.R., Hurlburt, W.W., Kostek, B., Gonder, D.S., Mastroeni, R.A., and Frail, D.E. (2001). Biochemical characterization of osteotesticular protein tyrosine phosphatase and its functional significance in rat primary osteoblasts. Biochemistry *40,* 814–821.

Destaing, O., Saltel, F., Geminard, J.C., Jurdic, P., and Bard, F. (2003). Podosomes display actin turnover and dynamic self-organization in osteoclasts expressing actin-green fluorescent protein. Mol. Biol. Cell *14,* 407–416.

Duong, L.T., Lakkakorpi, P.T., Nakamura, I., Machwate, M., Nagy, R.M., and Rodan, G.A. (1998). PYK2 in osteoclasts is an adhesion kinase, localized in the sealing zone, activated by ligation of alpha(v)beta3 integrin, and phosphorylated by src kinase. J. Clin. Invest. *102,* 881–892.

Elson, A. (1999). Protein tyrosine phosphatase epsilon increases the risk of mammary hyperplasia and mammary tumors in transgenic mice. Oncogene *18,* 7535–7542.

Elson, A., and Leder, P. (1995a). Protein-tyrosine phosphatase epsilon. An isoform specifically expressed in mouse mammary tumors initiated by v-Haras OR neu. J. Biol. Chem. *270,* 26116–26122.

Elson, A., and Leder, P. (1995b). Identification of a cytoplasmic, phorbol ester-inducible isoform of protein tyrosine phosphatase epsilon. Proc. Natl. Acad. Sci. USA *92,* 12235–12239.

Endo, N., Rutledge, S.J., Opas, E.E., Vogel, R., Rodan, G.A., and Schmidt, A. (1996). Human protein tyrosine phosphatase-sigma: alternative splicing and inhibition by bisphosphonates. J. Bone Miner. Res. *11,* 535–543.

Evans, J.G., Correia, I., Krasavina, O., Watson, N., and Matsudaira, P. (2003). Macrophage podosomes assemble at the leading lamella by growth and fragmentation. J. Cell Biol. *161,* 697–705.

Fisher, J.E., Rodan, G.A., and Reszka, A.A. (2000). *In vivo* effects of bisphosphonates on the osteoclast mevalonate pathway. Endocrinology *141,* 4793–4796.

Fisher, J.E. *et al.* (1999). Alendronate mechanism of action: geranylgeraniol, an intermediate in the mevalonate pathway, prevents inhibition of osteoclast formation, bone resorption, and kinase activation *in vitro.* Proc. Natl. Acad. Sci. USA *96,* 133–138.

Gil-Henn, H., and Elson, A. (2003). Tyrosine phosphatase epsilon activates Src and supports the transformed phenotype of Neu-induced mammary tumor cells. J. Biol. Chem. *278,* 15579–15586.

Gil-Henn, H., Volohonsky, G., and Elson, A. (2001). Regulation of protein-tyrosine phosphatases alpha and epsilon by calpain-mediated proteolytic. J. Biol. Chem. *276,* 31772–31779.

Gil-Henn, H., Volohonsky, G., Toledano-Katchalski, H., Gandre, S., and Elson, A. (2000). Generation of novel cytoplasmic forms of protein tyrosine phosphatase epsilon by proteolytic processing and translational control. Oncogene *19,* 4375–4384.

Horne, W.C., Neff, L., Chatterjee, D., Lomri, A., Levy, J.B., and Baron, R. (1992). Osteoclasts express high levels of pp60c-src in association with intracellular membranes. J. Cell Biol. *119,* 1003–1013.

Hunter, T. (1995). Protein kinases and phosphatases: the yin and yang of protein phosphorylation and signaling. Cell *80,* 225–236.

Krueger, N.X., Streuli, M., and Saito, H. (1990). Structural diversity and evolution of human receptor-like protein tyrosine phosphatases. EMBO J. *9,* 3241–3252.

Lakkakorpi, P.T., Bett, A.J., Lipfert, L., Rodan, G.A. Duong, le T. (2003). PYK2 autophosphorylation, but not kinase activity, is necessary for adhesion-induced association with c-Src, osteoclast spreading, and bone resorption. J. Biol. Chem. *278,* 11502–11512.

Lakkakorpi, P.T., and Vaananen, H.K. (1991). Kinetics of the osteoclast cytoskeleton during the resorption cycle in vitro. J. Bone Miner. Res. *6,* 817–826.

Li, L., and Dixon, J.E. (2000). Form, function, and regulation of protein tyrosine phosphatases and their involvement in human diseases. Semin. Immunol. *12,* 75–84.

Linder, S., and Aepfelbacher, M. (2003). Podosomes: adhesion hot-spots of invasive cells. Trends Cell Biol. *13,* 376–385.

Lowe, C., Yoneda, T., Boyce, B.F., Chen, H., Mundy, G.R., and Soriano, P. (1993). Osteopetrosis in Src-deficient mice is due to an autonomous defect of osteoclasts. Proc. Natl. Acad. Sci. USA *90,* 4485–4489.

Marchisio, P.C., Cirillo, D., Naldini, L., Primavera, M.V., Teti, A., and Zambonin-Zallone, A. (1984). Cell-substratum interaction of cultured avian osteoclasts is mediated by specific adhesion structures. J. Cell Biol. *99,* 1696–1705.

Marchisio, P.C., Cirillo, D., Teti, A., Zambonin-Zallone, A., and Tarone, G. (1987). Rous sarcoma virus-transformed fibroblasts and cells of monocytic origin display a peculiar dot-like organization of cytoskeletal proteins involved in microfilament-membrane interactions. Exp. Cell Res. *169,* 202–214.

Mauro, L.J., Olmsted, E.A., Davis, A.R., and Dixon, J.E. (1996). Parathyroid hormone regulates the expression of the receptor protein tyrosine phosphatase, OST-PTP, in rat osteoblast-like cells. Endocrinology *137,* 925–933.

Mauro, L.J., Olmsted, E.A., Skrobacz, B.M., Mourey, R.J., Davis, A.R., and Dixon, J.E. (1994). Identification of a hormonally regulated protein tyrosine phosphatase associated with bone and testicular differentiation. J. Biol. Chem. *269,* 30659–30667.

Missbach, M., Jeschke, M., Feyen, J., Muller, K., Glatt, M., Green, J., and Susa, M. (1999). A novel inhibitor of the tyrosine kinase Src suppresses phosphorylation of its major cellular substrates and reduces bone resorption *in vitro* and in rodent models *in vivo.* Bone *24,* 437–449.

Miyazaki, T., Neff, L., Tanaka, S., Horne, W.C., and Baron, R. (2003). Regulation of cytochrome c oxidase activity by c-Src in osteoclasts. J. Cell Biol. *160,* 709–718.

Moller, N.P., Moller, K.B., Lammers, R., Kharitonenkov, A., Hoppe, E., Wiberg, F.C., Sures, I., and Ullrich, A. (1995). Selective down-regulation of the insulin receptor signal by protein-tyrosine phosphatases alpha and epsilon. J. Biol. Chem. *270,* 23126–23131.

Murakami, H. *et al.* (1997). Tiludronate inhibits protein tyrosine phosphatase activity in osteoclasts. Bone *20,* 399–404.

Nakamura, K., Mizuno, Y., and Kikuchi, K. (1996). Molecular cloning of a novel cytoplasmic protein tyrosine phosphatase PTP epsilon. Biochem. Biophys. Res. Commun. *218,* 726–732.

NRC (National Research Council). (1996). Guide for the Care and Use of Laboratory Animals. National Academy Press, Washington, DC.

Nermut, M.V., Eason, P., Hirst, E.M.A., and Kellie, S. (1991). Cell/substratum adhesions in RSV-transformed rat fibroblasts. Exp. Cell Res. *193,* 382–397.

Opas, E.E., Rutledge, S.J., Golub, E., Stern, A., Zimolo, Z., Rodan, G.A., and Schmidt, A. (1997). Alendronate inhibition of protein-tyrosine-phosphatase-meg1. Biochem. Pharmacol. *54,* 721–727.

Parfitt, A.M., Drezner, M.K., Glorieux, F.H., Kanis, J.A., Malluche, H., Meunier, P.J., Ott, S.M., Recker, R.R. (1987). Bone histomorphometry: standardization of nomenclature, symbols, and units. Report of the ASBMR Histomorphometry Nomenclature Committee. J. Bone Miner. Res. *2,* 595–610.

Peretz, A., Gil-Henn, H., Sobko, A., Shinder, V., Attali, B., and Elson, A. (2000). Hypomyelination and increased activity of voltage-gated K(+) channels in mice lacking protein tyrosine phosphatase epsilon. EMBO J. *19,* 4036–4045.

Ponniah, S., Wang, D.Z., Lim, K.L., and Pallen, C.J. (1999). Targeted disruption of the tyrosine phosphatase PTPalpha leads to constitutive downregulation of the kinases Src and Fyn. Curr. Biol. *9,* 535–538.

Rogers, M.J., Gordon, S., Benford, H.L., Coxon, F.P., Luckman, S.P., Monkkonen, J., and Frith, J.C. (2000). Cellular and molecular mechanisms of action of bisphosphonates. Cancer *88,* 2961–2978.

Sanjay, A. *et al.* (2001). Cbl associates with Pyk2 and Src to regulate Src kinase activity, alpha(v)beta(3) integrin-mediated signaling, cell adhesion, and osteoclast motility. J. Cell Biol. *152,* 181–195.

Schmidt, A. *et al.* (1996). Protein-tyrosine phosphatase activity regulates osteoclast formation and function: inhibition by alendronate. Proc. Natl. Acad. Sci. USA *93,* 3068–3073.

Skorey, K., Ly, H.D., Kelly, J., Hammond, M., Ramachandran, C., Huang, Z., Gresser, M.J., and Wang, Q. (1997). How does alendronate inhibit protein-tyrosine phosphatases? J. Biol. Chem. *272,* 22472–22480.

Soriano, P., Montgomery, C., Geske, R., and Bradley, A. (1991). Targeted disruption of the c-src proto-oncogene leads to osteopetrosis in mice. Cell *64,* 693–702.

Stickel, S.K., and Wang, Y.L. (1987). Alpha-actinin-containing aggregates in transformed cells are highly dynamic structures. J. Cell Biol. *104,* 1521–1526.

Su, J., Muranjan, M., and Sap, J. (1999). Receptor protein tyrosine phosphatase alpha activates Src-family kinases and controls integrin-mediated responses in fibroblasts. Curr. Biol. *9,* 505–511.

Suhr, S.M., Pamula, S., Baylink, D.J., and Lau, K.H. (2001). Antisense oligodeoxynucleotide evidence that a unique osteoclastic protein-tyrosine phosphatase is essential for osteoclastic resorption. J. Bone Miner. Res. *16,* 1795–1803.

Sully, V., Pownall, S., Vincan, E., Bassal, S., Borowski, A.H., Hart, P.H., Rockman, S.P., and Phillips, W.A. (2001). Functional abnormalities in protein tyrosine phosphatase epsilon-deficient macrophages. Biochem. Biophys. Res. Commun. *286,* 184–188.

Tanuma, N., Nakamura, K., and Kikuchi, K. (1999). Distinct promoters control transmembrane and cytosolic protein tyrosine phosphatase epsilon expression during macrophage differentiation. Eur. J. Biochem. *259,* 46–54.

Tanuma, N., Nakamura, K., Shima, H., and Kikuchi, K. (2000). Protein-tyrosine phosphatase PTPepsilon C inhibits Jak-STAT signaling and differentiation induced by interleukin-6 and leukemia inhibitory factor in M1 leukemia cells. J. Biol. Chem. *275,* 28216–28221.

Tanuma, N., Shima, H., Nakamura, K., and Kikuchi, K. (2001). Protein tyrosine phosphatase epsilonC selectively inhibits interleukin-6- and interleukin-10-induced JAK-STAT signaling. Blood *98,* 3030–3034.

Tanuma, N., Shima, H., Shimada, S., and Kikuchi, K. (2003). Reduced tumorigenicity of murine leukemia cells expressing protein-tyrosine phosphatase, PTP epsilon C. Oncogene *22,* 1758–1762.

Tarone, G., Cirillo, D., Giancotti, F.G., Comoglio, P.M., and Marchisio, P.C. (1985). Rous sarcoma virus-transformed fibroblasts adhere primarily at discrete protrusions of the ventral membrane called podosomes. Exp. Cell Res. *159,* 141–157.

Toledano-Katchalski, H., Kraut, J., Sines, T., Granot-Attas, S., Shohat, G., Gil-Henn, H., Yung, Y., and Elson, A. (2003). Protein tyrosine phosphatase Epsilon inhibits signaling by mitogen-activated protein kinases. Mol. Cancer Res. *1,* 541–550.

Tonks, N.K., and Neel, B.G. (2001). Combinatorial control of the specificity of protein tyrosine phosphatases. Curr. Opin. Cell Biol. *13,* 182–195.

Umeda, S., Beamer, W.G., Takagi, K., Naito, M., Hayashi, S., Yonemitsu, H., Yi, T., and Shultz, L.D. (1999). Deficiency of SHP-1 protein-tyrosine phosphatase activity results in heightened osteoclast function and decreased bone density. Am. J. Pathol. *155,* 223–233.

Violette, S. M. *et al.* (2001). Bone-targeted Src SH2 inhibitors block Src cellular activity and osteoclast-mediated resorption. Bone *28,* 54–64.

Violette, S.M. *et al.* (2000). A Src SH2 selective binding compound inhibits osteoclast-mediated resorption. Chem. Biol. *7,* 225–235.

Wabakken, T., Hauge, H., Finne, E.F., Wiedlocha, A., and Aasheim, H.-C. (2002). Expression of human protein tyrosine phosphatase epsilon in leucocytes: a potential ERK pathway-regulating phosphatase. Scand. J. Immunol. *56,* 195–203.

Wu, L.W., Baylink, D.J., and Lau, K.H. (1996). Molecular cloning and expression of a unique rabbit osteoclastic phosphotyrosyl phosphatase. Biochem. J. *316,* 515–523.

Zambonin-Zallone, A., Teti, A., Carano, A., and Marchisio, P.C. (1988). The distribution of podosomes in osteoclasts cultured on bone laminae: effect of retinol. J. Bone Miner. Res. *3,* 517–523.

Zamir, E., Katz, B.Z., Aota, S., Yamada, K.M., Geiger, B., and Kam, Z. (1999). Molecular diversity of cell-matrix adhesions. J. Cell Sci. *112,* 1655–1169.

Zheng, X.M., Wang, Y., and Pallen, C.J. (1992). Cell transformation and activation of pp60c-src by overexpression of a protein tyrosine phosphatase. Nature *359,* 336–339.